Time constant optimization of solar irradiance absolute radiometer*

TANG Xiao (唐潇)[1,2,3], **FANG Wei** (方伟)[1]**, **WANG Yu-peng** (王玉鹏)[1], **YANG Dong-jun** (杨东军)[1], **and YI Xiao-long** (衣小龙)[1]

1. Changchun Institute of Optics, Fine Mechanics and Physics, Chinese Academy of Sciences, Changchun 130033, China

2. University of Chinese Academy of Sciences, Beijing 100049, China

3. School of Mechanical Engineering, University of South China, Hengyang 421001, China

(Received 18 November 2016; Revised 19 December 2016)

We experimentally evaluate and optimize the time constant of solar irradiance absolute radiometer (SIAR). The systemic error introduced by variable time constant is studied by a finite element method. The results shown that, with a classic time constant of 30 s for SIAR, the systemic errors are 0.06% in the midday and 0.275% in the morning and afternoon. The uncertainty level which can be considered negligible for SIAR is also investigated, and it is suggested that the uncertainty level has to be less than 0.02%. Then, combining the requirement of international comparison with these two conclusions, we conclude that the suitable time constant for SIAR is 20 s.

Document code: A **Article ID:** 1673-1905(2017)03-0179-5

DOI 10.1007/s11801-017-7032-7

The earth's climate and weather are ultimately driven by absorbed solar irradiance. So it is essential to measure the total solar irradiance (TSI) and monitor its variation to realize the global energy budget of the earth[1,2]. The reliable record of TSI began in 1978, when NIMBUS7 was launched with an absolute radiometer on board[3].

The absolute radiometer has been developed by Changchun Institute of Optics, Fine Mechanics and Physics (CIOMP) in China[4-7]. It was sent into space onboard the SHENZHOU-3 spacecraft from March to September in 2002. The discrepancy between our data and the data simultaneously measured by EOS/ACRIM is less than 0.2%[8]. In order to establish accurate and stable TSI database, a new package of solar irradiance absolute radiometer (SIAR) was sent into space onboard the FENGYUN-3C (FY-3C) polar orbiting meteorological satellite on 23 September 2013[9,10]. The SIAR was designed to measure the quantity of optical radiation in optical range from ultraviolet to far infrared[11], which covers the irradiance measurement range from 100 W/m^2 to 1 400 W/m^2 and the wavelength range from 0.2 μm to 50 μm using selectable gratings, and the measurement sensitivity of the SIAR is 0.2 W/m^2 [12].

The time constant of main cavity are critical for TSI measurement. For example, each satellite has various missions, and it is unsuitable for radiometers to operate its observational mission for days with bad weather, so the SIAR had to accomplish its launch mission in 8 days in 2013. It is too difficult to achieve adequate and useful data in such a short time. In order to shorten the time constant, the most meaningful method is to reduce the volume of main cavity. However, the sensitivity of the overall cavity absorptivity is exclusively dependent on the cavity geometry. It can be said that the smaller the cavity, the lower the cavity absorptivity, which has a direct impact on the measured accuracy of SIAR. In conclusion, there is a compromise to be found to optimize the time constant of SIAR.

The purpose of this paper is to explore the suitable time constant for SIAR. The systemic error introduced by variable time constant is studied by a finite element method.

The schematic diagram of SIAR is shown in Fig.1. The radiometer has two inverted cavities. One is the main cavity, and the other the compensation cavity for shielding the cavity temperature changes caused by the heat sink temperature fluctuation. Two cavities are installed together into the heat sink made of aluminum. The copper-constantan thermocouples contact the main cavity with the heat sink. It is designed to measure the temperature difference between main cavity and heat sink by thermoelectric effect. The resistive heating wires are embedded into the main cavity at the position where the solar radiation first strikes the cavity[13].

The main cavity consists of 24.3-mm-long silver cone with radius of 13 mm and central angle of 30°. The thickness of the cone wall is 0.06 mm. The inner surface of the cavity is coated with black paint, and the high absorbance

* This work has been supported by the National Natural Science Foundation of China (No.41474161), and the National High Technology Research and Development Program of China (No.2015AA123703).

** E-mail: tanggxiao1022@126.com

of the black paint and multiple reflections make the absorption efficiency close to 1. The main aperture is located behind the view-limiting aperture, and a series of apertures are located between these two apertures to prevent the drift driven by scatting light. The optical path takes advantage of those from other absoluter radiometer[14,15].

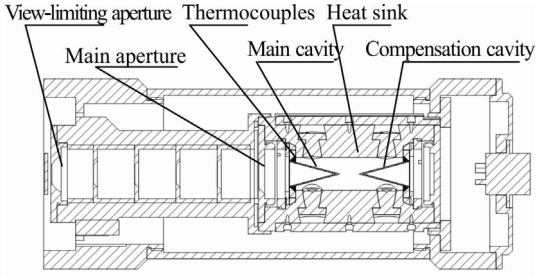

Fig.1 The schematic diagram of SIAR

The basic operation procedure of SIAR consists of three processes, which are self-test process, solar measurement process, and electrical substitution process[16,17].

In self-test process, close the shutter, and apply a low electrical power P_L and a high electrical power P_H in main cavity, respectively. The thermocouples detect the temperature difference between main cavity and heat sink in each state, and the equilibrium value (T_L and T_H) are outputted. Then, the sensitivity of the main cavity calibration by electrical power is given by

$$S = \frac{P_H - P_L}{T_H - T_L}. \tag{1}$$

In solar measurement process, open the shutter, and apply another low electrical power P_1 simultaneously to prevent the rapid temperature response of main cavity. The absorbed radiant power P_0 and low electrical power P_1 maintain the temperature difference at T_1.

In electrical substitution process, close the shutter again. Compute an electrical power P_2 with the sensitivity of main cavity S to keep the temperature difference stabilizing at the same value T_1. Because of the non-equivalence between radiant heating and electrical heating, the temperature difference maintain at T_2 actually. Then, the absorbed radiant power is given by

$$P_0 = P_2 - P_1 - S(T_2 - T_1). \tag{2}$$

Given the absorption of main cavity of α[18,19] and the measured area of main aperture of A_m[20,21], the measured solar irradiance is given by

$$E = \frac{P_0}{\alpha A_m} f, \tag{3}$$

where f is the product of other correction factors, e.g., correction factor for the sun-earth distance and correction factor for traceability.

As mentioned before, the measurement of TSI is important for earth's climate. However, this physical quantity is only adequate for space-based measurements, whereas it is called as direct solar radiation (DSR) on the ground. In order to eliminate the relative system error between absolute radiometers, it is necessary to set up the international comparison experiment of DSR.

Fig.2 shows the measurement of DSR over a day in Davos (Switzerland), two SIAR-series radiometers are setup, and both of them share the same design. The relative error between two radiometers is less than 0.25%, which shows the good repeatability of SIAR. Fig.3 shows the rate of change for DSR over a measurement day. The change of DSR is more obvious in the morning and afternoon. In the morning, the DSR is raised by 2 $W \cdot m^{-2} \cdot min^{-1}$, and in the afternoon, it is decreased at a rate more than 2 $W \cdot m^{-2} \cdot min^{-1}$. However, in the midday, the signal is almost constant at a stable level, the change is small as 0.15 $W \cdot m^{-2} \cdot min^{-1}$ from fraction 0.47 to 0.53.

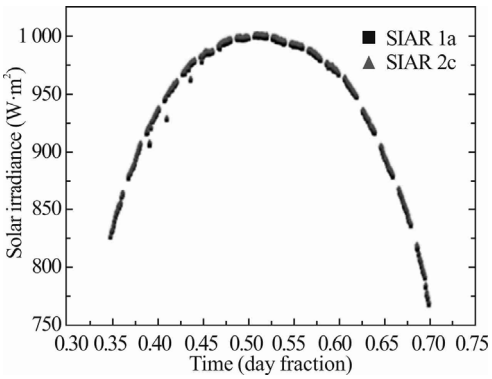

Fig.2 DSR measurement result over a day in Davos (Switzerland)

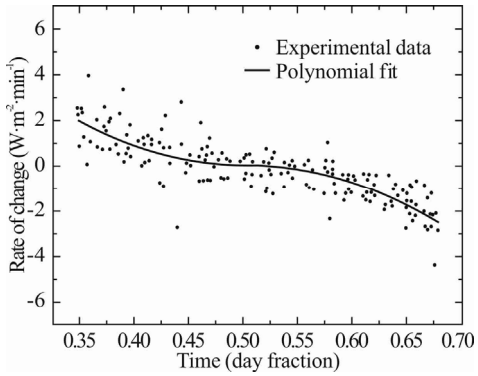

Fig.3 The rate of DSR change over a day in Davos (Switzerland)

Because of different environments for the measurements of DSR and TSI, some additional requirements need to be taken into consideration. For example, when measuring the solar radiation on the ground, the radiometers must be able to adapt changes in the irradiation level. The change in DSR over a day could introduce a systematic error if the time constant is too slow. This requirement will be analyzed in the next section.

The finite element method is a powerful and flexible tool to model the complex three-dimensional system. Here, we establish the finite element model of heat transfer system of SIAR, which takes advantage of bilateral symmetry and consists of 23 404 elements and 18 840

nodes, as shown in Fig.4. Because the radiometer is maintained at an ultrahigh vacuum circumstance (less than 1×10^{-5} Pa), the convection through air is neglected in this modeling. For element finite method, the governing equation is

$$(C)\{\dot{\boldsymbol{T}}\}+(K)\{\boldsymbol{T}\}=\{\dot{\boldsymbol{Q}}\}, \quad (4)$$

where $\boldsymbol{T}$ and □ are the vectors of the nodal temperature and its time derivate, and $\dot{\boldsymbol{Q}}$ is the heating power vector, which accounts for the heat flow across the boundary. Variable thermophysical properties are input to the finite element system as tables of discrete data points. The program then calculates properties as specific temperatures by linear interpolation between the given data points.

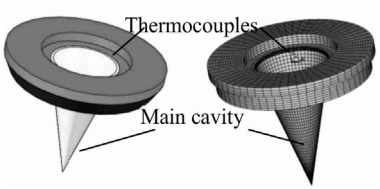

Fig.4 The gridded model of heat transfer system of SIAR

In order to estimate the accuracy and correctness of the results obtained by the finite element method, we observe the dependence of final temperature difference between main cavity and heat sink on input powers. The results are compared with the obtained experimental results, as shown in Fig.5. The discrepancy, which is less than 0.14%, shows that the experimental results and numerical model agree well. The observed disagreement can be attributed to the uncertainties in the modeling, such as the geometry and material properties. It will be taken into consideration when determining the overall uncertainty of TSI measurement.

With the results obtained from Fig.5 by using the linear interpolation, it is possible to predict the input power from the temperature difference between main cavity and heat sink, and this power level is regarded as "measured power" in following. However, because of the change of DSR, the "measured power" is not equal to the "true power".

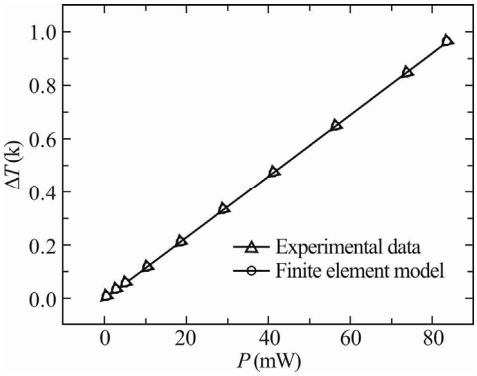

Fig.5 Temperature difference between main cavity and heat sink of the radiometer versus input power compared with finite element model data

Because DSR is changing over time, there will be a measurement error between the "true power" and "measured power". In order to estimate this error, we apply the increased input power to the model. Fig.6 shows the step response of the main cavity model, which starts at 1 365 W/m^2 (the solar irradiance standard in world radiation reference) and is increased by a rate of 2 W·m^{-2}·min^{-1}. Thus, the function with input power starting at 1 365 W/m^2 and increased by 2 W·m^{-2}·min^{-1} can produce the "true power", whereas the "measured power" can be obtained from the given temperature difference and linear interpolation.

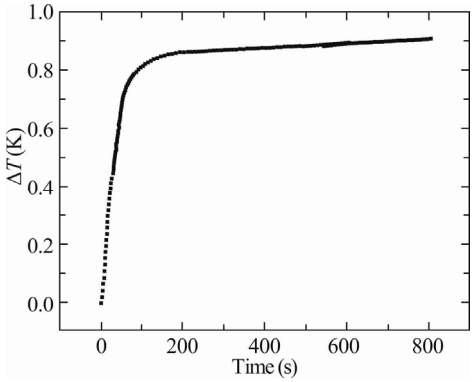

Fig.6 The step response of the main cavity model starting at 1 365 W/m^2 and increased by a rate of 2 W·m^{-2}·min^{-1}

Fig.7 shows relative errors between the "true power" and "measured power" with a classic time constant of 30 s. In Fig.7, different increased rates of 0.15 W·m^{-2}·min^{-1}, 0.3 W·m^{-2}·min^{-1}, 0.45 W·m^{-2}·min^{-1}, 0.6 W·m^{-2}·min^{-1}, 1 W·m^{-2}·min^{-1} and 2 W·m^{-2}·min^{-1} are applied at the incident area. Combined with Fig.3, it shows that in the morning, the relative error due to change of DSR is about 0.275%, and it is approximately more than −0.275% in the afternoon, and small as 0.060% in the midday.

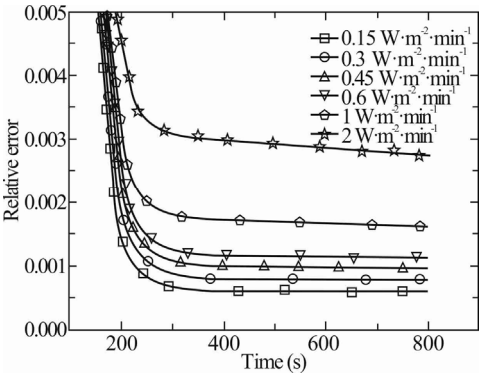

Fig.7 Relative errors between the "true power" and "measured power" with a classic time constant of 30 s

Tab.1 shows the detailed standard uncertainties with various time constants and rates of change. The relative uncertainties are deduced from the relative errors. For

example, the relative error with change rate of 2 $W \cdot m^{-2} \cdot min^{-1}$ and time constant of 30 s is 0.275%. The value can be seen as the maximum boundary *h*. Therefore, the value ranges from 0 to *h*. Such a distribution is usually regarded as a "rectangular probably distribution", and the standard uncertainty of the value is given by[22]

$$\mu = \frac{h}{2} / \sqrt{3} . \tag{5}$$

So the standard uncertainty with change rate of 2 $W \cdot m^{-2} \cdot min^{-1}$ and time constant of 30 s is 0.079%.

Tab.1 Standard uncertainties with various time constants and rates of change (The negligible uncertainties are shown in bold.)

Time constant	Standard uncertainty for different change rates ($W \cdot m^{-2} \cdot min^{-1}$)					
(s)	0.15	0.3	0.45	0.6	1	2
5	**0.012%**	**0.012%**	**0.013%**	**0.013%**	**0.014%**	**0.015%**
10	**0.013%**	**0.014%**	**0.016%**	**0.017%**	**0.020%**	0.028%
15	**0.014%**	**0.017%**	**0.019%**	0.021%	0.027%	0.041%
20	**0.015%**	**0.019%**	0.022%	0.025%	0.034%	0.054%
25	**0.016%**	0.021%	0.025%	0.029%	0.040%	0.066%
30	**0.017%**	0.023%	0.028%	0.035%	0.047%	0.079%

There are two factors to impact the selection and optimization of suitable time constant of SIAR. The first is the uncertainty threshold, i.e., the uncertainty can be considered negligible for SIAR when it is less than the threshold, and the other is the requirement of international comparison in Dovas.

For an instrument as complex as SIAR, it is necessary to know how small an individual uncertainty to be ignored with respect to the combined uncertainty. The combined uncertainty is calculated as[20]

$$u_c = \sqrt{\sum_{i=1}^{N} u^2(x_i)} . \tag{6}$$

Fig.8 shows the combined uncertainty of SIAR, which is set as an initial overall uncertainty of 0.2% (the target overall uncertainty of SIAR) plus different tiny uncertainties u_t of 0.01%, 0.02%, 0.03%, 0.04% and 0.05%.

It is a reasonable assumption that there will be more than 10 tiny uncertainty components which can be considered negligible for a precise instrument, like SIAR. It can be observed from Fig.8 that only the situation with $u_t \leq 0.02\%$ is most suitable for the uncertainty analysis. The increased combined uncertainty will be less than 0.01% when the number of additional tiny uncertainties is 10. Meanwhile, even when the number of additional tiny components is unrealistically increased to 100, the increased combined uncertainty is still significantly small than 0.1%. In summary, for SIAR, an individual uncertainty component can be considered negligible if it does not exceed 0.02%. Therefore, the uncertainty levels which accord with this requirement are shown in bold in Tab.1.

As we know, because of different cavity geometries and various components, there must be a systemic error for every absolute radiometer. Therefore, every five years (in 2005, 2010, 2015), World Radiant Center (WRC) in Davos held the international comparison to offset this error[8,23]. In order to improve efficiency of international comparison, a successful requirement was suggested by professor Finsterle, which is that the least effective measurement data should be 50 in one day for absolute radiometer during the comparison period[24]. For SIAR, it takes about 1.5 min to record one point, and has to take a rest for 9 min after record every 13 points. That is to say, 13 points can be registered every 30.5 min which equals to day fraction of 0.021 with 24 h being regarded as 1. For completing the measurement requirement for international comparison with 50 points in one day, the minimum consume time for a measurement day is a variation of day fraction of 0.081.

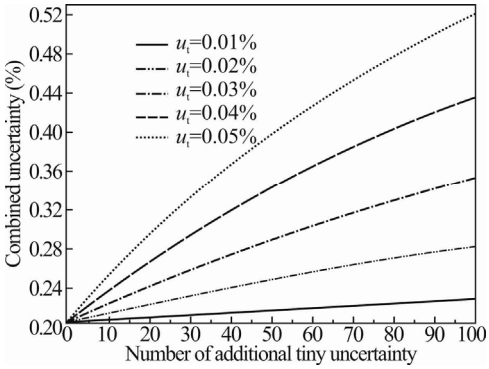

Fig.8 Combined uncertainty of SIAR, assuming an overall uncertainty of 0.2% plus variable number of tiny uncertainty components

Tab.2 shows the range and variation of day fraction with various change rates. The range of day fraction is deduced from the results of Fig.4. For the requirement of minimum variation of day fraction of 0.081, the suitable change range of DSR is from −0.3 $W \cdot m^{-2} \cdot min^{-1}$ to 0.3 $W \cdot m^{-2} \cdot min^{-1}$.

Tab.2 Range and variation of day fraction with various change range of DSR

Change range of DSR ($W \cdot m^{-2} \cdot min^{-1}$)	Range of day fraction	Variation of day fraction
−0.15—0.15	0.473—0.531	0.058
−0.3—0.3	0.451—0.555	0.104
−0.45—0.45	0.434—0.573	0.139
−0.6—0.6	0.421—0.588	0.167
−1—1	0.394—0.617	0.223
−2—2	0.351—0.661	0.310

In summary, considering these two impact factors and using the given results from Tab.1, we suggest that the minimum uncertainty which can be considered negligible for the change rate of 0.3 $W \cdot m^{-2} \cdot min^{-1}$ is 0.019%. Then it is concluded that the suitable time constant for SIAR is 20 s.

In conclusion, accurate measurements of solar irradiance require meaningful selections of time constant. In this paper, we set up the experiment of DSR measurement in Davos. It is shown that maximum change rate for DSR is observed in the morning or afternoon. For example, with a classic time constant of 30 s, the DSR is raised by 2 $W \cdot m^{-2} \cdot min^{-1}$ in the morning, and is decreases with a rate more than 2 $W \cdot m^{-2} \cdot min^{-1}$ in the afternoon, whereas the change rate is small as 0.15 $W \cdot m^{-2} \cdot min^{-1}$ in the midday.

Because of the change of DSR, the time constant of SIAR needs to be optimized. Therefore, the finite element model is employed to study the steady state and transient response of the main cavity. The finite element model agrees well with experimental data within 0.14%. It is also used to estimate the extra systemic error introduced by variable time constant. The results suggest that, with considering the combination of the requirement for accuracy and international comparison, the suitable time constant for SIAR is 20 s.

References

[1] G. Kopp, A. Fehlmann, W. Finsterle, D. Harber, K. Heuerman and R. Wilson, Metrologia **49**, S29 (2012).

[2] T. Pulli, T. Donsberg, T. Poikonen, F. Manoocheri, P. Karha and E. Ikonen, Light: Science & Applications **4**, e332 (2015).

[3] H. Kyle, D. Hoyt and J. Hickey, Solar Physics **152**, 9 (1994).

[4] Y. Wang, X. Hu, H. Wang, X. Ye and W. Fang, Optics and Precision Engineering **23**, 1807 (2015). (in Chinese)

[5] D.Yang, W.Fang, X.Ye and B. Song, Optics and Precision Engineering **23**, 1813 (2015). (in Chinese)

[6] B. Song, X. Ye, D. Yang, M. Jiang and W. Fang, Optics and Precision Engineering **23**, 1903 (2015). (in Chinese)

[7] X. Tang, W. Fang and Y. Wang, Chinese Journal of Lasers **43**, 0408003 (2016).

[8] W. Fang, B. Yu, H. Yao, Z. Li, C. Gong and X. Jin, Acta Optica Sinica **23**, 112 (2003). (in Chinese)

[9] H. Wang, H. Li, and W. Fang, Applied Optics **53**, 1718 (2014).

[10] Z. Yang, N. Lu, J Shi, P Zhang, C Dong and J. Yang, IEEE Transaction on Geoscience and Remote Sensing **50**, 4846 (2012).

[11] A. Rogalski and K. Chrzanowski, Metrology and Measurement Systems **21**, 565 (2014).

[12] W. Fang, H. Wang, H. Li and Y. Wang, Solar Physics **289**, 4711 (2014).

[13] Z. Yang, W. Fang, Y. Luo and Z. Xia, Chinese Optics Letters **12**, 101202 (2014).

[14] W. Pang, X. Zheng, J. Li, X. Shi, H. Wu, M. Xia, D. Gao, J. Shi, T. Qi and Q. Kang, Chinese Optics Letters **13**, 051201 (2015).

[15] G. Kopp and G. Lawrence, Solar Physics **230**, 91 (2005).

[16] X. Tang, W. Fang, Y. Luo, K. Wang and Z. Xia, Acta Optica Sinica **36**, 1012004 (2016). (in Chinese)

[17] X. Tang, P. Jia, K. Wang, B. Song, W. Fang and Y. Wang, Optics and Precision Engineering **24**, 2370 (2016). (in Chinese)

[18] Q. Fang, Research of the Blackbody Cavity and Nonequivalence of Spatial Cryogenic Radiometer, University of Chinese Academy of Sciences, (2014).

[19] Q. Fang, W. Fang, Z. Yang, B. Yu and H. Hu, Metrologia **49**, 572 (2012).

[20] X. Chen, W. Fang, Y. Wang, Z. Yang and X. Quan, Acta Optica Sinica **35**, 0912003 (2015). (in Chinese)

[21] J. Fedchak, A. Carter and R. Datla, Metrologia **43**, S41 (2006).

[22] JCG Metrology, Evaluation of Measurement Data — Guide to the Expression of Uncertainty in Measurement, (2008).

[23] W. Finsterle, P. Blattner, S. Moebus, I. Ruedi, C. Wehrli, M. White and W. Schmutz, Metrologia **45**, 377 (2008).

[24] W. Finsterle, WMO International Pyrheliometer Comparison IPC-XFinal Report, (2011).